Journal of Applied Polymer Science

Migration of Additives Toward the Surface During Aging of Epoxy Coating by Infrared Spectroscopy

Keli Du,[1] Guang Yang,[1] Zehong Yuan,[1] Wen Xu,[2] Xiaofan Liang[2]

[1]Key Laboratory of Aerospace Advanced Materials and Performance (Ministry of Education), School of Materials Science and Engineering, Beihang University, Beijing 100191, China

[2]Aerospace Research Institute of Materials and Processing Technology, Beijing 100076, China

Correspondence to: G. Yang (E-mail: yangguang@buaa.edu.cn)

ABSTRACT: This research highlights the application of multi-angle attenuated total reflection (ATR) infrared (IR) spectroscopy method in investigating the migration of additives from the bulk toward the surface which happens in the epoxy coating. Concentration profiles of additives such as low molecular polyamide 651 (LMPA 651) and 2,4,6 - tris (dimethylaminomethyl) phenol (DMP-30) were studied. Analysis of the shape of the additives concentration profiles revealed the existence of enrichment region and indicated the migration phenomenon of additives in epoxy coating during natural aging and accelerated aging processes. The changes of the additives concentration determined by the ATR-IR method were consistent with the results obtained by FTIR analysis and gravimetric analysis. The result shows that the ATR-IR method is very promising for investigating the surface chemical changes in epoxy coating due to its nondestructive testing, conveniency, and high efficiency. © 2013 Wiley Periodicals, Inc. J. Appl. Polym. Sci. **2014**, *131*, 40051.

KEYWORDS: ageing; spectroscopy; coatings

Received 25 August 2013; accepted 13 October 2013

DOI: 10.1002/app.40051

INTRODUCTION

Epoxy resin materials are widely used in many applications such as adhesives and coatings in aerospace and automobile engineering.[1,2] One of the major concerns about this polymer is the long-term stability. A lot of work has been done in both natural aging and accelerated aging processes. The aging behaviors usually include the physical aging[3,4] such as structural relaxation and chemical aging[5–8] mainly involving intermolecular chemical structure changes. However, the work concerning the surface migration of molecular during the aging processes which can also lead to performance degradation has not been reported widely. The migration of additives in the polymer matrix is influenced by their size and structure, the morphology, property of the polymer and the conditions of operation such as temperature and pressure of the internal medium. Buch[9] suggested that there was a migration of nitrogen- and sulphur-containing molecules from bulk toward the surface during the thermal degradation of a modified epoxy adhesive. And results also strongly indicated that the molecules which migrated to the surface were indeed the cross-linking agents. Merlatti[10] used FTIR, PyGC-MS, and DMA to characterize multi-layers coating degradation during artificial cycling tests. In his research, based and primer binder formulated with dibutylphtalate as a plasticizer were found to evolve strongly with a rise in T_g of the epoxy binder as high as 40°C.

There are many characterization methods employed in investigation of the surface properties such as optical electron microscopy analysis,[11,12] AES,[13,14] AFM,[15–17] SIMS,[18] and XPS,[19,20] etc. However, all of these measurements can only obtain information of the very surface or nanometer scale sub-surface.[21] In many cases, the information obtained from the very thin surface layer is incomplete. Instead, extended depth of surface layer and its concentration changes have attracted much attention in recent years.

Among surface techniques, ATR-IR spectroscopy is one of the most popular methods for surface characterization especially in the field of polymer science.[22,23] As a surface method, its advantage is the ability to give much information on the surface such as chemical composition and structure, orientation and conformation, crystallinity, hydrogen bonding, etc.[24] The IR spectra measured by an ATR configuration with various incident angles demonstrate information of the functional groups on the depth distribution from the surface to about a micrometer under the surface.[25] Some research had been done based on ATR[26,27] and multi-angle ATR[24,28] methods. Nagai[29] demonstrated the photo-degradation appearing from the surface to the

depth in micro-scale in some polymers by simulating the angle resolved ATR spectra phenomenologically. Vitali[30] estimated the surface concentration increase with time by means of utilizing mathematically corrected ATR spectra, which made it possible to get a surface concentration of additives.

In addition, infrared spectrometer subtract technology is a method to analysis the ATR spectra according to the obtained difference spectrum. The subtraction of two spectra, or difference spectroscopy, which is sensitive to all types of band changes, provides a straightforward way to simplify an experimental spectrum and/or extracting overlapping bands.[31] It can reflect the intensity changes of all characteristic peaks between two IR spectra in one spectrum intuitively.[32] In a difference spectrum, it is easy to visualize the changes in the spectra caused by internal (chemical reaction) or external (temperature, pressure, concentration, pH, etc.) perturbations. However, it is not widely used and only some research reported this method.[33,34]

This article describes the application of ATR-IR and difference spectrum to the characterization of additives migration which exists in epoxy coating surface during natural aging and accelerated thermal-oxidation aging. As shown in this study, the concentration profile analysis of additives migration is important for investigating the components characteristics of surface.

EXPERIMENTAL

Materials and Preparation

Diglycidyl ether of bisphenol-A (DGEBA) and novolacs epoxy resin (EPN) were purchased from Wuxi Resin Factory (China), and cured with a combination of low molecular polyamide 651 (LMPA 651) and 2,4,6 - tris (dimethylaminomethyl) phenol (DMP-30) from Tianjin Chemical Company (China). The epoxy values of DGEBA and EPN are both 0.51 mol/100 g. The weight composition of the epoxy coating is 42% of polymer matrix and 58% of other additives.

Quantitative DGEBA and EPN were first heated respectively in air oven at 55°C, 15 min, and then mixed to form a homogeneous blend. The mixture of DGEBA and EPN were vacuated at 80°C about 15 min to remove the residual air bubbles in the system. Then, the vacuated mixture of LMPA 651 and DMP-30 was added slowly to get a well-distributed mixing resin. At last, the blend was poured in molds with glass substrate of dimensions 30 × 8 × 1 mm^3. The moldings were cured in air oven at 65°C for 4 h.

The samples of cured epoxy coating were aged respectively at ambient atmosphere (20 ± 2°C) to carry on natural aging for 40 days and at 50°C thermal-oxidation aging in ventilated oven for 30 days, ESPEC facility (Japan) H201. And one half amounts of the samples' surfaces were covered by glasses.

ATR-IR Analysis

We performed ATR measurements with different angles of incidence on the samples. The spectrometer used for these measurements was a Nexus-470 instrument equipped with a variable incident angle ATR accessory (VeeMAX II). ZnSe was chosen as the internal reflection prism and the angles of incidence selected were 40°, 40.5°, 41°, 43°, and 45°, respectively. ATR spectra were collected in the range of 4000–400 cm^{-1}. The resolution was 4 cm^{-1} with 32 accumulated scans.

The basic ATR method is that IR light above the critical angle shows a total internally reflection at the interface crystal/sample. The light containing chemical information exits from the crystal and passes through the spectrometer to the detector.[35] The spectral intensity depends on the depth of penetration of the evanescent wave from the crystal into the sample. The formula for the depth is given by:[36]

$$d_p = \frac{\lambda}{2\pi n_1 \left(\sin^2\theta - n_{21}^2\right)^{1/2}} \quad (1)$$

where λ is the wavelength of incident light, θ is the angle of incidence of infrared light, n_1 is the refractive indices of prism, and n_{21} is n_2/n_1, where n_2 is the refractive indices of sample ($n_1 = 2.43$, $n_2 = 1.51$).

In fact, some factors such as angle of incidence, the wavelength of incident light and index of refraction might affect the ATR spectra and then introduced some distortions into spectra. Therefore, it was of great importance to conduct the ATR correction. The advanced ATR correction algorithm from OMNIC software could correct the band intensity distortion, peak shifts, and nonpolarization effects.[37,38]

Difference spectrum obtained by subtraction two different ATR spectra of different incident angles from the OMNIC software. For example, the spectrum of 40° incident angle was subtracted from the spectrum of 40.5° incident angle and the different spectrum was marked as 40–40.5°.

FTIR Analysis

Fourier transform infrared (FTIR) spectra were carried out with a Nexus-470 spectrophotometer. The spectra were recorded from 4000 cm^{-1} to 400 cm^{-1} and 32 scans were averaged for a resolution of 4 cm^{-1}. The sample was carefully scraped from the surface of epoxy coating. Plates were made from a mixture of the sample and KBr power and then analyzed in transmittance mode.

Gravimetric Analysis

Samples were allowed to cool from the test temperature to ambient for 30 min in a desiccator. Percentage relative mass lose, $\eta(T, t)$, is given simply by formula (2):

$$\eta(T_i, t_j) = \frac{\Delta m}{m_0} \times 100 = \frac{m_{ij} - m_0}{m_0} \times 100 \quad (2)$$

where m_0 is the initial sample weight, m_{ij} is the weight of aged sample, T_i and t_j are aging temperature and aging time respectively.

DSC Analysis

Differential Scanning Calorimerty (DSC) analysis was performed by using STA 449F3 (NETZSCH, Germany) to obtain the curing exothermic enthalpy. In this study, the specimens were sampled with a mass of about 5 mg. The temperature range varied from ambient to 200°C at a heating rate of 5°C/min.

RESULTS AND DISCUSSION

Approach Background

By substituting parameters into the eq. (1), the penetration depth ranges from the sub-micrometer to micro-meter order.

Table I. The Depth of Penetration Corresponds with Different Incidence Angle

θ (°)	40	40.5	41	43	45
Depth (μm)	4.5	3.4	2.8	1.9	1.5

Usually, the depth of penetration as well as the intensity increases with the decreases of incident angle.[39,40] Therefore, we can obtain the multi-angle ATR spectra of different depths by changing the incident angles. In this research, the angles of incidence selected are 40°, 40.5°, 41°, 43°, and 45°, respectively. The depth penetration of each angle is shown in Table I. The ATR spectra at multiple angles of incidence of cured epoxy coating are shown in Figure 1.

As shown in Table I, it can be seen clearly that the penetration depth increased with the decrease of incidence angle. And Figure 1 reveals that the intensity increases with the decreases of incident angle.

The difference spectra of ATR spectra at multiple incident angles of cured epoxy coating are shown in Figure 2. The absorbance intensity in difference spectrum of 40–40.5° can represent the concentration changes of the intermediate layer from 4.5 to 3.4 μm.

The component concentration is determined by calculating the relative absorbance of absorption bands as A/A_0, where A_0 is the internal standard. In this study, the C—H bending vibration peak of methyl group at 1361 cm^{-1} is taken as the internal standard. By this method, we can obtain the concentration change of each depth layer. Figure 3 shows the concentration changes of the absorption band at 3015 cm^{-1} in different depth regions of cured epoxy coating.

Infrared Analysis of Additives

FTIR and DSC analysis about curing process of epoxy coating are shown in Figures 4 and 5. After curing 4 h at 65°C, the oxirane rings with absorption at 916 cm^{-1} are consumed and disappear finally (Figure 4). Meanwhile, the relative intensities

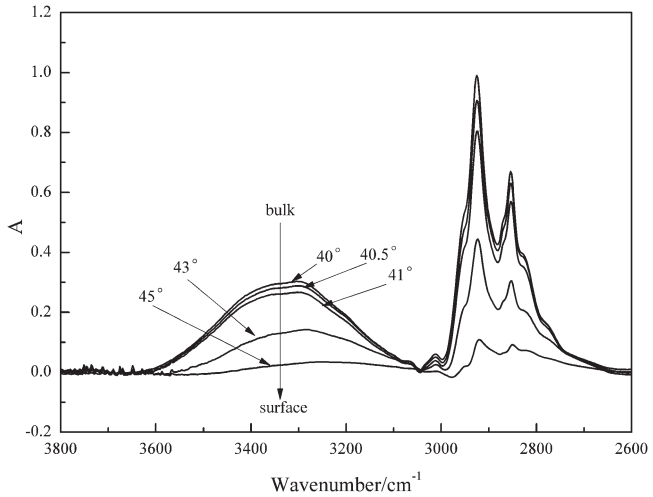

Figure 1. ATR spectra with multiple angles of incidence of cured epoxy coating.

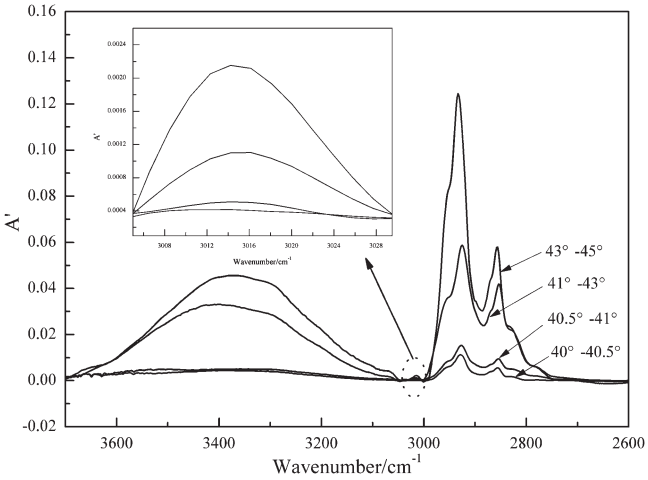

Figure 2. Difference spectra of cured epoxy coating.

increase as bands near 1115 cm^{-1} (stretching vibration of C—O in secondary alcohol) and 1036 cm^{-1} (stretching vibration of C—N in tertiary amine). The scheme of epoxy resin curing was

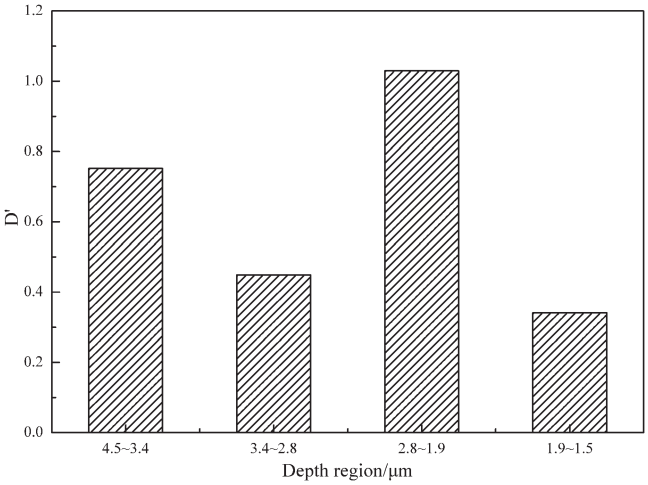

Figure 3. Concentration changes of band at 3015 cm^{-1}.

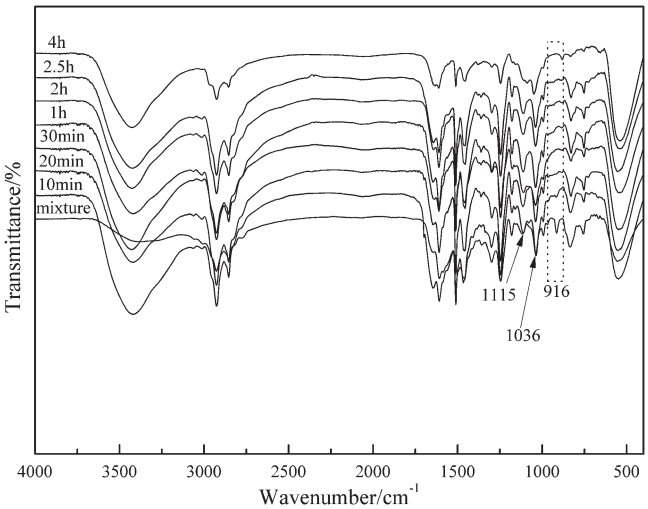

Figure 4. FTIR spectra of epoxy system at different curing stages.

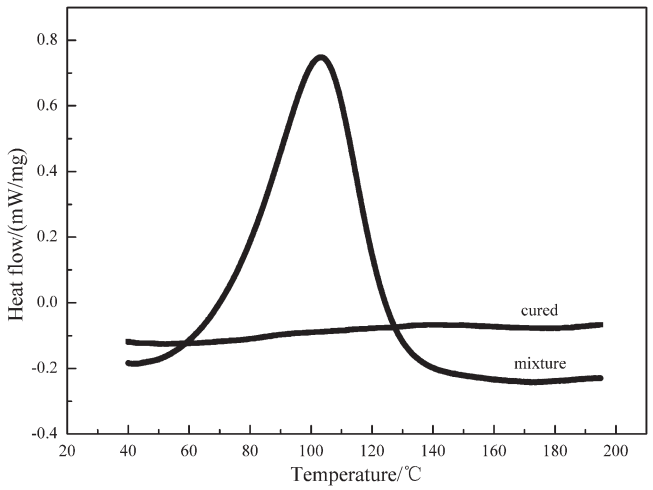

Figure 5. DSC curves of epoxy system before and after curing.

summarized in literature.[41] In addition, the exothermic peak disappears and the DSC curve is sub-horizontal after cured (Figure 5). FTIR and DSC results demonstrate that the epoxy had cured completely. It also shows that additives are excessive according to the stoichiometric calculations.

As the epoxy coating cured completely, it contains residual additives such as LMPA 651 and DMP-30. The existence of unreacted additives can also be confirmed by FTIR as shown in Figure 6. The assignments of the characteristic absorption bands of additives in the difference spectrum are shown in Table II.

According to Table II and Figure 6, the presentence of additives in epoxy coating can be confirmed as LMPA 651 (characteristic absorption bands such as in 3420, 3015, 1610, 1645, and 1298 cm^{-1}) and DMP-30 (characteristic absorption bands such as in 3423, 1610, 1183, and 1034 cm^{-1}).

Besides, each additive has its unique absorption band in the difference spectrum. The absorption band near 1645 cm^{-1} (the stretching vibration of C═O in amide) indicates the existence

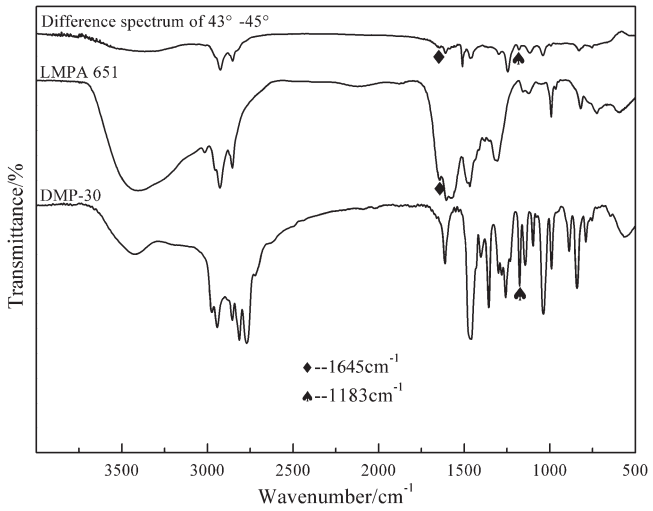

Figure 6. The difference spectrum of 43–45° and FTIR spectra of LMPA 651 and DMP-30.

Table II. Assignments of the Characteristic Absorption Bands in Difference Spectrum

Absorption bands (cm^{-1})	Assignment
3500-3300	Stretching vibration of N—H
3015	Stretching vibration of N—H in amide
1645	Stretching vibration of C═O in amide
1610	Stretching vibration of C═C skeleton in benzene ring
1298	Wagging vibration of C—H in methylene
1183	Stretching vibration of C—O in phenol
1034	Stretching vibration of C—N in primary amine

of LMPA 651. And the absorption band near 1183 cm^{-1} (the stretching vibration of C—O in phenol) can stand for DMP-30. The concentration changes of additives are represented by relative intensity of absorption bands in the difference spectrum of different intermediate layers and 1361 cm^{-1} is taken as internal standard as mentioned above. The concentration profiles of additives in cured epoxy coating act as benchmark. Thanks to this approach, the concentrations changes of additives with depth under different conditions will be obtained.

Concentration Profiles of Additives in Natural Aged Epoxy Coating

The natural aging condition is mild and the chemical aging does not occur during the short aging time as 40 days which can be demonstrated by FTIR analysis (not shown). Therefore, it is appropriate to investigate the migration phenomenon simply without chemical aging reactions. Figure 7 shows the concentration profiles of additives in epoxy coating after natural aging for 40 days. It exhibits increased concentrations after natural aging 40 days and reveals that the superfluous additives keep moving toward the surface. The concentration profiles comparison with cured epoxy coating is demonstrated in Figure 8. Then the typical enrichment in the region from 2.8 μm to 1.9 μm is observed in both the natural aging and the cured samples near the surface.

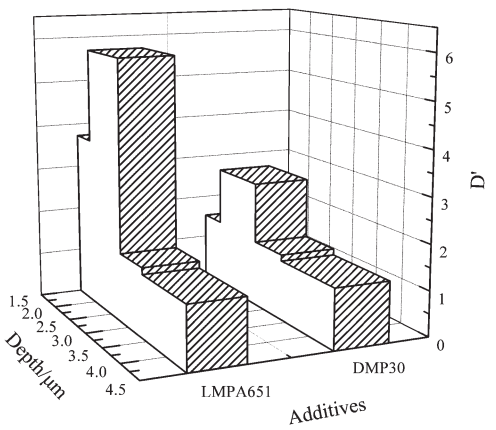

Figure 7. Concentration profiles of additives in natural aged epoxy coating.

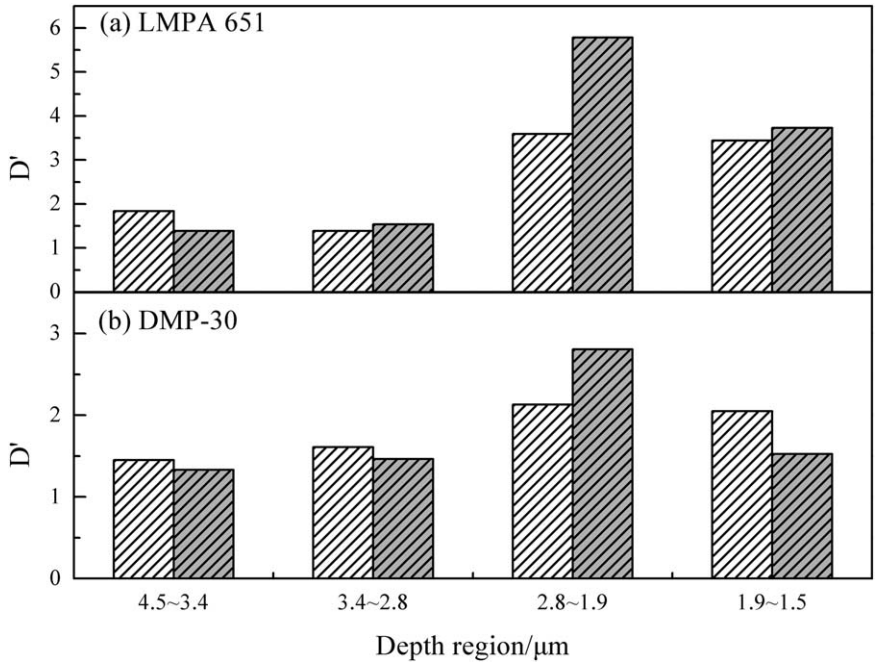

Figure 8. Comparison of concentration profiles of additives between cured (white bars) and natural aged (light gray bars) epoxy coatings.

As shown in Figure 8, there are also two main differences of the concentration changes between cured and natural aging samples. On the one hand, the concentration of each additive increases gradually from the depth of 4.5 to 2.8 μm in the aged sample. On the other hand, there is a sharp decrease of concentrations in the aged sample from 1.9 μm toward 1.5 μm which is much more apparent than the cured sample. The excessive additives remaining in the epoxy resin act as plasticizers whose migration is a well-documented phenomenon. The migration of additives in a polymer is a dynamic process so that the concentration value in a certain depth range is actually an average of a continuously varying amount.[30] And the additives to air/coating surface can be understood in terms of the need of the lowest surface free energy component of the coating to migrate toward the air/coating surface.

By the way, a slow evaporation might take place and leads to the decrease of additive concentration. After natural aging for 40 days, the additives molecules may transform into volatiles by air. This would explain the existence of a maximum near the surface and not at the surface.

Concentration Profiles of Additives in Accelerated Aged Epoxy Coating

The cured epoxy coating performs the thermal-oxidation aging at 50°C. During the thermal aging, there is chemical aging that can change the chemical structures and components after aging for long time.[42,43] However, it shows an induction period at the first several days of aging while the chemical aging phenomenon is not so obvious or doesn't occur at all.[44] To avoid the oxidation influence on migration analysis, the sample aging for 3 days is chosen to investigate the concentration profile. By FTIR analysis (not shown), it also can be proved that the chemical aging is nonexistence indeed in the sample.

Figure 9 shows the concentration profiles of additives in epoxy coating aging at 50°C for 3 days. It is evident that there is also a concentration maximum because of migration of additives. The main difference for the observed maxima in accelerated aging sample and natural aging sample is the locations of maxima. It can be seen in Figure 9 that the concentration maximum region is from 3.4 μm to 2.8 μm depth in the accelerated aging sample while the natural aging sample is from 2.8 μm to 1.9 μm. After thermal aging at 50°C for 3 days, the depth of enrichment region increases up to about 0.9 μm.

The positions of these maxima result from the difference between rate of migration of the additives toward the surface and the rate of volatilization of these additives.[9] The migration of additives is somewhat slower than the rate of volatilization

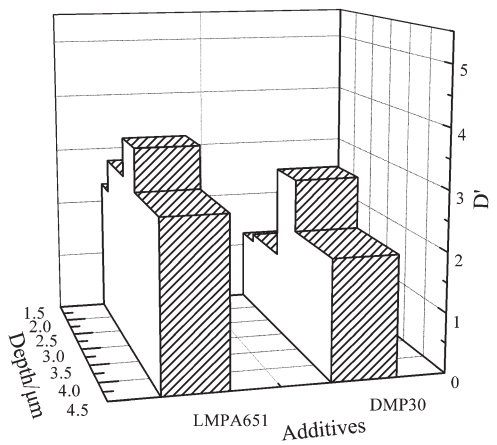

Figure 9. Concentration profiles of additives in epoxy coating of thermal-oxidation aging at 50°C for 3 days.

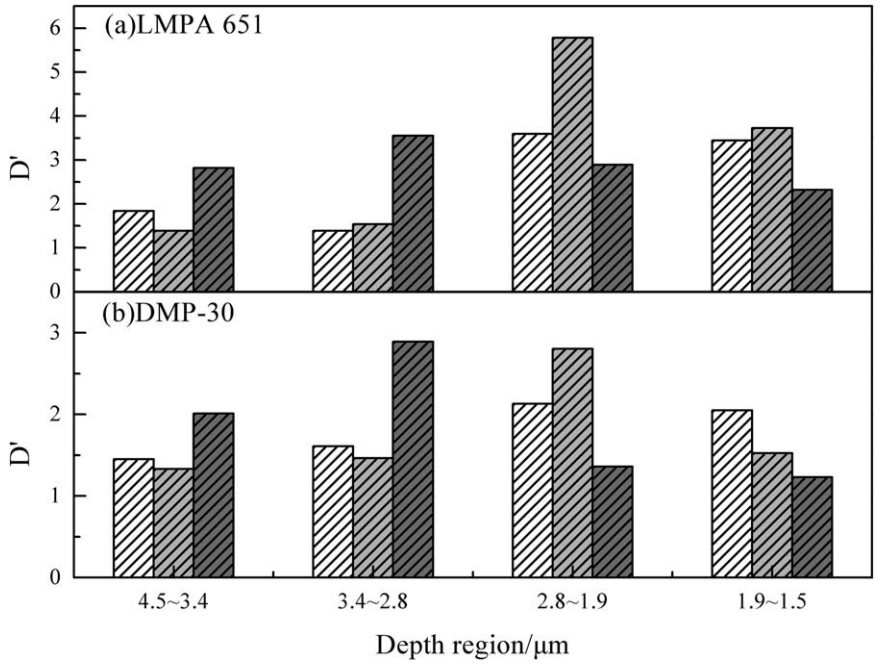

Figure 10. Comparison of concentration profiles of additives among cured (white bars), natural aged (light gray bars), and accelerated aged (gray bars) epoxy coatings.

and this could explain the observed shift of the enrichment region away from the sample surface to bulk. Then, there are concentration gradients of additives from 2.8 μm to 1.5 μm containing two depth regions. It suggests that raising the temperature of aging leads to a uniformly acceleration of migration as well as loss of additives. The explanation is also in agreement with the Arrhenius law of thermally active movement at higher temperature.[45]

The comparison of concentration profiles of different additives in epoxy coatings after cured, natural aging for 40 days and thermal-oxidation aging at 50°C for 3 days is demonstrated in Figure 10. And Figure 10(a) is the concentration profile of LMPA 651. It shows that, in the sample of thermal-oxidation aging at 50°C for 3 days, the concentration of LMPA 651 increases gradually in the first two depth regions to a maximum, higher than the samples suffering other two conditions as cured and natural aging. Then the concentration deceases by degrees and is lower than the other two conditions as well. The phenomenon repeatedly demonstrates the promotion of migration and volatilization at elevated temperature. In addition, additive concentration of DMP-30 changes similarly as shown in Figure 10(b), which suggests several dynamic processes happen. The additives must firstly migrate from the bulk at a certain rate and then it vacates the position and volatizes from the air/coating surface. Such migration phenomena based on the molecular mobility and the minimization of surface tension may have profound implications for the scientists and engineers engaged in formulating coatings and paints.[46]

As mentioned above, the samples were divided into two groups: one group was covered by glass while the other was not, although they were under the same aging condition. In order to verify the volatilization of additives in aged samples, we compared the weight of the samples from the two groups. As shown in Figure 11, the mass loss of sample covered by glass is only 0.05% after aging for 3 days, while the mass loss of the open sample is 0.19%. Since the aging time is short (only 3 days), there isn't obvious chemical reactions that can affect the mass of sample. Then it is proved that the loss of additives is a physical process as volatilization. Actually, the process of removal of any additive contains two distinct processes.[47] Initially, the additives volatilize from the coating surface, which will lead to a concentration gradient near the surface. Subsequently, the additives depleted from the surface will be replaced by additives migrating from the bulk. The phenomenon is found to be consistent with concentration profile previously analyzed.

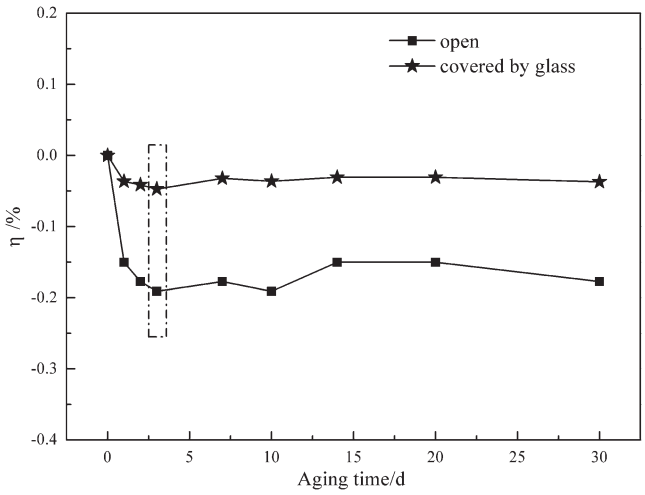

Figure 11. Mass loss ratios of epoxy coatings with and without glass on the surface over aging time at 50°C.

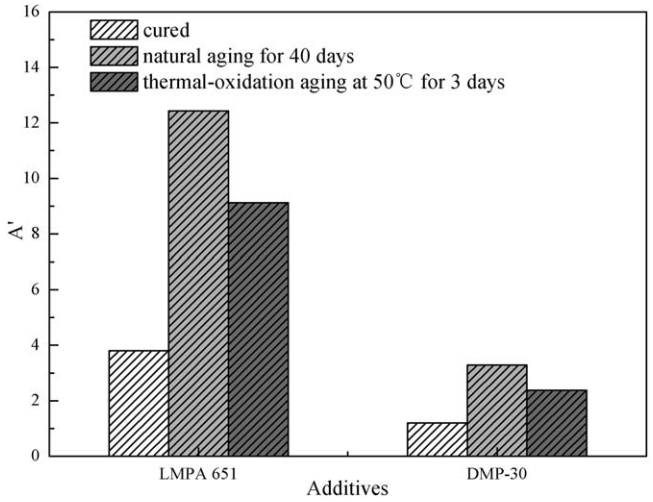

Figure 12. The concentrations of additives in epoxy coatings of cured (white bars), natural aging for 40 days (light gray bars) and thermal-oxidation aging at 50°C for 3 days (gray bars) by FTIR analysis.

Furthermore, the average concentrations near the surface of additives are measured from the FTIR spectra. The samples of cured, natural aging for 40 days and 50°C thermal-oxidation aging for 3 days are analyzed and the result is shown in Figure 12. It clearly reveals that the average concentrations of the two additives in the sample of natural aging for 40 days are higher than the cured sample. It indicates that the prolonged aging time definitely facilitates the migration. Similarly, the concentrations of additives in the sample of thermal-oxidation aging at 50°C for 3 days are higher than the cured sample but lower than the natural aged sample which suggests that the elevated temperature accelerates the rate of migration but also the volatilization. However, all of the suggestions still can't conceal the fact that the effect on migration is dominated.

Therefore, prolonged time and elevated temperature are the two main driving forces which influence the concentration changes. An increase of the driving forces accelerates the additives migration at the inner epoxy coating as well as volatilization.

CONCLUSIONS

The concentration profiles of additives migration of LMPA 651 and DMP-30 in epoxy coating are investigated by multi-angle ATR spectra and difference spectra. A method for semi-quantifying ATR absorbance intensity of additives in the epoxy substrates has been proposed. The concentration shape suggests that an enrichment layer of additives appears near the surface region. The concentration maximum position of sample after natural aging for 40 days is from 2.8 to 1.9 μm while the sample after 50°C thermal-oxidation aging for 3 days is from 3.4 μm to 2.8 μm. The accumulated layer of additives is supposed to be the interaction of molecular migration from the bulk to the surface and volatilization. The different positions of concentration maxima result from the rate difference between migration of additives toward surface and volatilization. Prolonged time and elevated temperature are proved to be the two main driving forces influencing the concentrations changes. The FTIR and gravimetric analysis results also indicate the phenomena of migration and volatilization. The technique demonstrated in this research to investigate the additives concentration profiles will be helpful in understanding the components changes of epoxy coating.

REFERENCES

1. Unnikrishnan, K. P.; Thachil, E. T. *Polym-Plast. Technol.* **2006**, *45*, 469.
2. Tomuta, A. M.; Ramis, X.; Ferrando, F.; Serra, A. *Prog. Org. Coat.* **2012**, *74*, 59.
3. Fata, D.; Possart, W. *J. Appl. Polym. Sci.* **2006**, *99*, 2726.
4. Odegard, G. M.; Bandyopadhyay, A. *J. Polym. Sci. Part B: Polym. Phys.* **2011**, *49*, 1695.
5. Alessi, S.; Conduruta, D. *Polym. Degrad. Stab.* **2010**, *95*, 677.
6. Clemens, B.; Davis, F.; Wulff, P. *J. Appl. Polym. Sci.* **2004**, *91*, 369.
7. Xiao, G.; Shanahan, M. E. R. *J. Appl. Polym. Sci.* **1998**, *69*, 363.
8. Pei, Y.; Wang, K.; Zhan, M.; Xu, W.; Ding. X. *Polym. Degrad. Stab.* **2011**, *96*, 1179.
9. Buch, X.; Shanahan, M. E. R. *Int. J. Adhes. Adhes.* **2003**, *23*, 261.
10. Merlatti, C.; Perrin, F. X.; Aragon, E.; Margaillan, A. *Prog. Org. Coat.* **2008**, *61*, 53.
11. Ghanbari-Siahkali, A.; Mitra, S.; Kingshott, P.; Almdal, K.; Bloch, C.; Rehmeier, H. K. *Polym. Degrad. Stab.* **2005**, *90*, 471.
12. Lin, S. S. *Surf. Interface. Anal.* **1987**, *10*, 110.
13. Ames, D. P.; Chelli, S. J. *Surf. Coat. Technol.* **2004**, *187*, 199.
14. Fitzgerald, A. G. *J. Microsc.* **1993**, *170*, 97.
15. Malwela, T.; Ray, S. S. *Polymer* **2012**, *53*, 2705.
16. Rezende, C. A.; Lee, L. T.; Galembeck, F. *Langmuir* **2009**, *25*, 9938.
17. Sarac, A. S.; Tofail, S. A. M.; Serantoni, M.; Henry, J.; Cunnane, V. J.; McMonagle, J. B. *Appl. Surf. Sci.* **2004**, *222*, 148.
18. Deimel, M.; Rulle, H.; Liebing, V.; Benninghoven, A. *Appl. Surf. Sci.* **1998**, *134*, 271.
19. Chandra, A.; Turng, L. S.; Gopalan, P.; Rowell, R. M.; Gong, S. *Compos. Sci. Technol.* **2008**, *68*, 768.
20. Duan, Y.; Pearce, E. M.; Kwei, T. K. *Macromolecules* **2001**, *34*, 6761.
21. Wild, R. K. *Adv. Mater. Opt. Electr.* **1995**, *5*, 53.
22. Laroche, G.; Fitremann, J.; Gherardi, N. *Appl. Surf. Sci.* **2013**, *273*, 632.
23. Nagai, N.; Hashimoto, H. *Appl. Surf. Sci.* **2001**, *172*, 307.
24. Koji, O.; Iwamoto, R. *Anal. Chem.* **1985**, *57*, 2491.
25. Nagai, N.; Okumura, H.; Imai, T.; Nishiyama, I. *Polym. Degrad. Stab.* **2003**, *81*, 491.
26. So, C. L.; Eberhardt, T. L.; Hsu, E.; Via, B. K.; Hse, C. Y. *J. Appl. Polym. Sci.* **2007**, *105*, 733.

27. Roberge, S.; Dubé, M. A. *J. Appl. Polym. Sci.* **2007**, *103*, 46.
28. Gulminea, J. V.; Janissek, P. R.; Heisec, H. M.; Akcelrudd, L. *Polym. Degrad. Stab.* **2003**, *79*, 358.
29. Nagai, N.; Matsunobe, T.; Imai, T. *Polym. Degrad. Stab.* **2005**, *88*, 224.
30. Vitali, M. *Polym. Test.* **2001**, *20*, 741.
31. Grdadolnik, J. *Vib. Spectrosc.* **2003**, *31*, 279.
32. Grdadolnik, J.; Maréchal, Y. *Vib. Spectrosc.* **2003**, *31*, 289.
33. Masayo, I.; Jacques, B.; Peter, R. R. *BBA.* **2002**, *1555*, 116.
34. Okubo, T.; Noguchi, T. *Spectrochim. Acta A.* **2007**, *66*, 863.
35. Tuyet-Trinh, D.; Mathew, C.; Peter, M. F. *Polym. Degrad. Stab.* **2002**, *77*, 417.
36. Harrick, N. *J. Ann. NY. Acad. Sci.* **1963**, *101*, 928.
37. Linh, T. C. C.; Le, H.; John, R.; David, A. B. *Langmuir* **2008**, *24*, 8036.
38. Swedlund, P. J.; Miskelly, G. M.; McQuillan, A. J. *Langmuir* **2010**, *26*, 3394.
39. Hamid, S. H.; Prichard, W. H. *Polym.-Plast. Technol.* **1988**, *27*, 303.
40. Haller, G. L.; Rice, R. W.; Wan, Z. C. *Catal. Rev.* **1976**, *13*, 259.
41. Karayannidou, E. G.; Achilias, D. S.; Sideridou, I. D. *Eur. Polym. J.* **2006**, *42*, 3311.
42. Bockenheimer, C.; Fata, D.; Possart, W. *J. Appl. Polym. Sci.* **2004**, *91*, 361.
43. Fuente, J. L. *Polym. Degrad. Stab.* **2009**, *94*, 664.
44. Galant, C.; Fayolle, B.; Kuntz, M.; Verdu, J. *Prog. Org. Coat.* **2010**, *69*, 322.
45. Geertz, G.; Brüll, R.; Wieser, J.; Maria, R.; Wenzel, M.; Engelsing, K.; Wüst, J.; Bastian, M.; Rudschuck, M. *Polym. Degrad. Stab.* **2009**, *94*, 1092.
46. Hinder, S. J.; Lowe, C.; Maxted, J. T.; Watts, J. F. *Prog. Org. Coat.* **2005**, *54*, 104.
47. Calvert, P. D.; Billingham, N. C. *J. Appl. Polym. Sci.* **1979**, *24*, 357.